CHAPTER V
ELECTRICAL RESPONSIVE MATERIAL BASED POLYCARBAZOLE/ ALGINATE BIO-HYDROGEL COMPOSITE AS AN ACTUATOR

5.1 Abstract

Actuator is a mechanical device for displacing a system component under some kind of energy. For the actuating applications, it should provide a large deformation under activated energy. Generally, electric field is often used to induce material deformation and certain electroactive polymers can offer large modulus responses under electric field. The aims of this work are to study the electromechanical properties of sodium alginate (SA) hydrogel and polycarbazole/sodium alginate (PCB/SA) hydrogel blend under the influence of the electric field strength. The electromechanical properties of pristine SA were studied under effects of crosslinking types and SA molecular weights. The electromechanical properties of PCB/ SA blends were studied under the effect of PCB concentrations. The electromechanical properties of the pristine SA as crosslinked by the ionic crosslinking agent were higher than those of the covalent crosslinking. Moreover, the electromechanical responses of SA increased with increasing molecular weight. Finally, the electromechanical response of the SA/PCB blend was the highest at 0.10 %v/v PCB which provided the storage modulus sensitivity of 18.5 under applied electric field strength of 800 V/mm.

Keywords: Sodium alginate hydrogel, Biocompatible actuator, Electromechanical properties, Polycarbazole.

5.2 Introduction

Polymer artificial muscle technology is being developed for large deformations by repetitive molecular motions. Polymer artificial muscles have been divided into two major groups (Mirfakhrai *et al.*, 2007). The first group is an electronic electroactive polymers (EAPs) in which the dimensional changes occur in response to an electric field, for example: piezoelectric polymer (Mirfakhrai *et al.*,

2007). The second group is an ionic electroactive polymers (DEAs) (Mirfakhrai *et al.*, 2007) in which the movement of ions is required to make an actuation possible, for examples: conductive polymers, polymer gels. The applications of artificial muscles are developed for animals, human, and the creation of human-like robots. Electroactive conductive polymers can be used to enhance the electrical and mechanical responses where biopolymers are used as the matrix phase.

Alginates are natural anionic biopolymers extracted from brown seaweeds. They are unbranched polysaccharide consisting of 1,4-linked b-D- mannuronic acid and a-L-guluronic acid units (Kuen *et al.*, 2012). Alginates have been extensively investigated and used for many biomedical applications, due to its biocompatibility, low toxicity, relatively low cost, and they can be prepared through gelation method at room temperature (Kuen *et al.*, 2012. Hydrogels are three dimensionally crosslinked networks composed of hydrophilic polymers with high water content. Chemical or physical crosslinking of hydrophilic polymers are typical approaches to form hydrogels, and their physicochemical properties are highly dependent on the crosslinking type and crosslinking density, in addition to the molecular weight and chemical composition of the polymers.

Polycarbazole is one of the conductive polymers that contain two six-membered benzene ring fused on side of a five-membered nitrogen containing ring. It is synthesized through either electrochemical or chemical method (Gupta and Prakash *et al.*, 2010). Mostly, it can be used in the applications of light-emitting diodes, electrochromic displays, organic transistors, and rechargeable batteries (Harun *et al.*, 2007; Gupta *et al.*, 2010; and Raj *et al.*, 2010) due to it is high conductivity.

In this work, we are interested in fabricating an electroactive material from alginate in a form of hydrogel as the matrix phase filled with polycarbazole. A small amount of polycarbazole was added as a dispersed phase to improve the electrical and electromechanical properties of the alginate hydrogel. It is of interest to study the alginate hydrogels and alginate/polycarbazole hydrogel blends for an actuator application.

5.3 Experimental

5.3.1 Materials

Carbazole monomer as monomer and citric acid as a covalent crosslinking agent were purchased from Merck. Ammonium persulphate as an oxidizing agent, sodium alginates with different molecular weights as a matrix, Tween 20 as a surfactant were purchased from Sigma-Aldrich. Dichloromethane as a solvent, sodium dodecyl sulfate (SDS) as a surfactant, perchloric acid as a doping agent, hydrochloric acid as a solvent were purchased from RCI Labscan. Cetyl trimethylammonium bromide (CTAB) as a surfactant, calcium chloride as an ionic crosslinking were purchased from Fluka.

5.3.2 Characterizations and Testing

5.3.2.1 Fourier Transform Infrared Spectrometer

A Fourier Transform Infrared Spectrometer, FT-IR (Nicolet, Nexus 670) was used to characterize the functional group of SA film. This technique was used to identify the absorption modes with 32 scans and a resolution of ± 4 cm^{-1}, covering a wavelength range of 4000-400 cm^{-1}.

5.3.2.2 X-ray Diffractometer

An X-ray diffractometer, XRD (Rigaku) was used to investigate the amount of crystallinity in the hydrogel samples. The diffractometer was operated in the Bragg-Brentano geometry and fitted with a graphite monochromator and the diffracted beam using a 5°/min scan rate.

5.3.2.3 Thermal Gravimetric Analyzer

A thermal gravimetric analyzer (DuPont, TGA 2950) was used to determine amount of moisture content and the decomposition temperatures of SA hydrogels. The thermal behavior was investigated by weighting sample of 5-10 mg, placing it in a platinum pan, and then heating it under nitrogen flow with a heating rate of 10°C/min from 30-800°C.

5.3.2.4 Scanning Electron Microscope

A Scanning Electron Microscope, SEM (Hitachi, S4800) was used to examine the morphological structure of the dispersion of PCB in SA hydrogels. The samples were attached on to a brass-stub. Prior to observation, samples were gold sputtered.

5.3.2.5 Atomic Force Microscope

An Atomic Force microscope, AFM (CSPM) images were taken to determine the topology of the hydrogels of various crosslinking types and concentrations of PCB by using a scan rate 0.5 Hz and a scan size of 2.5 × 2.5 μm^2.

5.3.2.6 Crosslinking Density

The crosslinking density of hydrogel was analyzed by the swelling method of Gudeman and Peppas (1995). A sample of the hydrogel (1 cm^2 square) was cut and weighed in air and heptane (a non-solvent). The sample was placed in a stainless steel mesh basket which was suspended in heptane to obtain the accurate weight measurements in heptane. The sample was then placed in a buffer solution for 5 days to reach equilibrium, and then was weighed in air and heptane again. Finally, the sample was dried at 25 °C in a vacuum for 5 days. Once again, it was weighed in air and heptane. M_c, the average weight between crosslinks, was calculated from Equation 5.1:

$$\frac{1}{\overline{M}_c} = \frac{1}{\overline{M}_n} - \frac{\frac{\bar{v}}{V_1}\left[\ln\left(1-v_{2,s}\right)+v_{2,s}+\chi_1 v_{2,s}^2\right]}{v_{2,r}\left[\left(\frac{v_{2,s}}{v_{2,r}}\right)^{1/3}-\frac{1}{2}\left(\frac{v_{2,s}}{v_{2,r}}\right)\right]} \qquad (5.1)$$

where $\overline{M}_n$ is the number-average molecular weight of the polymer before cross-linking, $\bar{v}$ is the specific volume of alginate ($\bar{v}$ =0.60 cm^3/g of alginate), $\overline{V}_1$ is the molar volume of water (18.1 cm3/mol), $v_{2,r}$ is the volume fraction of the polymer in a relaxed state, $v_{2,s}$ is the volume fraction of the polymer in solvent state, χ_1 is the Flory polymer-solvent interaction parameter of alginate (χ_1 for alginate is 0.473).

5.3.2.7 Electromechanical Properties

The electromechanical properties of the SA hydrogels were investigated in terms of electric field strength. A melt rheometer (Rheometric Scientific, ARES) was fitted with a parallel plate fixture (diameter of 25 mm). A DC voltage was applied with a DC power supply (Instek, GFG8216A). A digital multimeter was used to monitor the voltage input. In these experiments, the oscillatory shear mode was applied and the dynamic moduli (G' and G") were measured as functions of frequency and electric field strength. Strain sweep tests was first carried out to determine the suitable strains to measure G' and G" in the linear viscoelastic regime. The frequency sweep tests was carried out to measure G' and G" of each sample as functions of frequency. The frequency was varied from 0.1 to 100 rad/s. Prior to each measurement, the SA hydrogel samples were pre-sheared at a low frequency under an electric field for 15 min to ensure the formation of equilibrium polarization before the G' and G" measurements. Experiments were carried out at the temperature of 300 K and repeated at least two or three times. The temporal response experiments were also carried out at 800 V/mm. For the electromechanical properties of PCB/SA hydrogel composites, it was carried out with the same procedure as the pristine SA hydrogels.

5.3.2.8 Dielectrophoresis Forces

The dielectrophoresis forces of the SA hydrogel and its composites were determined by measuring the deflection distances of the specimens in the vertical cantilever fixture under electric field. The specimens were vertically immersed in the silicone oil (viscosity=100 cSt) between parallel copper electrode plates (68 mm of length, 40 mm of width, and 2 mm of thickness). The gap between the pair of the electrodes was 30 mm. A DC voltage was applied with a DC power supply (Goldsun, GPS 3003B) connected to a high voltage power supply (Gamma High Voltage, UC5-30P and UC5-30N). A video camera was used to record the movement during experiment. Pictures were captured from the video and the deflection distances in x (d) and y axes (l) at the end of the specimen and determined by using the Scion Image software (version 4.0.3). The electric field strength was varied between 0 and 500 V/mm at the room temperature of 300 K. Both the voltage

and the current were monitored. The resisting elastic force of the specimens were calculated under electric field using the non-linear deflection theory of a cantilever, which was obtained from the standard curve between $(F_e l_0^2)/(El)$ and d/l_0 (l_0 = initial length of specimens); F_e is the elastic force, d is the deflection distance in the horizontal axis, l is the deflection distance in the vertical axis, E is the Young's modulus which is equal to $2G'(1+\nu)$, where G' is the shear storage modulus taken to be G' (ω = 1 rad/s) at various electric field strength and I is the moment of inertia $1/12t^3w$, where t is the thickness of the sample and w is the width of the sample. The electrophoresis force was calculated from the static horizontal force balance consisting of the elastic force, the corrective gravity force (mgtanθ), and the buoyancy force ($\rho vgtan\theta$) as shown in Equation (5.2):

$$F_d \approx F_e + mg(\tan\theta) - \rho Vg(\tan\theta) \qquad (5.2)$$

where g is 9.8 m/s^2, m is the mass of the specimen, and θ is the deflection angle, ρ is the density of the fluid (silicon oil = 0.97g/cm^3), V is the volume of the displaced of fluid.

5.3.3 Preparation of SA Hydrogel

SA solutions with three molecular weights as low molecular weight SA (LSA) of 2.83×10^5 g/mol, medium molecular weight SA (MSA) of 3.34×10^5 g/mol, and high molecular weight SA (HSA) 4.57×10^5 g/mol in distilled water (1.0%v/v) were prepared at room temperature under continuous stirring for 40 min. (Kulkarni *et al.*, 1999). The crosslinking of SA was carried out by the ionic and covalent crosslinking methods (Kuen *et al.*, 2012). In case of the ionic crosslinking method, it was prepared by adding the appropriate volume of $CaCl_2$ solution to the SA solution at room temperature under continuous stirring for 30 min with $CaCl_2$ concentrations varying from 0.0050, 0.0100, 0.0150, 2.0, and 0.0200 %v/v. In case of the covalent method, it was prepared by adding the appropriate volume of citric acid solution to the SA solution at 80°C under continuous stirring for 30 min with

citric acid concentration varying from 0.25, 0.50, 0.75, and 1.0 %v/v. Both of SA mixture solutions were poured into plastic petri dishes (10 cm of diameter). The SA hydrogels were obtained after allowing water evaporation at room temperature for a period of 2 days and kept at 4°C for controlling water content within the SA hydrogels.

5.3.4 Preparation of PCB/SA Hydrogel Composites

The polycarbazole synthesized with adding of CTAB via interfacial polymerization method (Gupta *et al.*, 2010) was dispersed into 70 ml SA solution filled with crosslinking agent. The concentration of PCB was varied from 0.01, 0.05, 0.1, 0.5, 1.0, 3.0, and 5.0 %v/v. The solution was poured into a plastic Petri dish for casting at room temperature for 2 days to get the hydrogel composites.

5.4 Results and Discussion

5.4.1 Crosslinking Density of SA Hydrogel

The crosslinked SA hydrogels were prepared by two different crosslinking methods which were the ionic crosslinking from calcium chloride ($CaCl_2$) and the covalent crosslinking from citric acid (CA). Table 5.1 shows the crosslinking density of SA hydrogels of various $CaCl_2$ and CA concentrations.

With increasing crosslinking concentration, the crosslinking density of SA hydrogels continuously increases because of a higher probability of the crosslinking agent to form SA hydrogel network (Paradee *et al.*, 2012).

In the case of SA hydrogels crosslinked with $CaCl_2$, the crosslinking density increases by a factor of two when increasing $CaCl_2$ concentration from 0.005 to 0.02 %v/v. For the effect of SA molecular weight, a lower molecular weight SA possesses a higher crosslinking density compared with the others because a shorter molecular chain has a larger free volume and chain ends that facilitate an easy attachment between the Ca^{2+} ions and the functional groups of SA (Stone *et al.*, 2013). Similarly, the crosslinking density of SA hydrogels crosslinked with CA increases with CA concentration by about 8 times when increasing SA concentration from 0.25 to 1.00 %v/v.

Comparing the effect of crosslinking method, the CA system provides a higher crosslinking density than the $CaCl_2$ system because the carboxyl group of CA molecule can permanently react with the carboxyl group of SA molecule as a chemical bonding (Stone *et al.*, 2013). While Ca^{2+} ions from a physical bond with SA molecule. When crosslinked SA hydrogels were swollen in the water for evaluating the crosslinking density, the physical bond was easily destroyed and water can easily penetrate through the specimens causing a large amount of weight loss (Kuen *et. al.*, 2012).

The crosslinking densities of SA hydrogels from the two crosslinking methods are nearly at 0.015%v/v of $CaCl_2$ and 0.50%v/v of CA. The values are in the range of 15×10^{-6} to 20×10^{-6} mol/cm^3. Thus, these two samples were used in the further studies.

5.4.2 Fourier Transform Infrared Spectroscope

SA hydrogels were prepared by the crosslinking agents through either the ionic crosslinking (adding of $CaCl_2$) or covalent crosslinking (adding of CA), and were first characterized for the functional groups by the FT-IR technique.

The characteristic FT-IR spectrum of HSA hydrogels, as shown in Figure 5.2 (a), indicates the peak of the O-H stretching at 3265 cm^{-1}, the -COO$^-$ at 1590-1587 cm^{-1}, the C-C and C-O stretching at 1771 cm^{-1}, the C-C stretching at 1025 cm^{-1}, and the C-H stretching at 800-815 cm^{-1} (Saarai *et al.*, 2013). As can be observed, the positions of the -COO$^-$ and O-H bands shift and the vibration intensity apparently decreases with the addition of $CaCl_2$ (Figure 5.2 (b)) which implies that both the -COO$^-$ and O-H groups on SA molecules had been preferentially coordinated with calcium ions (Ca_2^+) in the $CaCl_2$ solution (Wang *et al.*, 2010). Moreover, the positions of the -COO$^-$ and O-H bands shift and the vibration intensity apparently decreases with the addition of CA (Figure 5.2 (c)) which implies that both the -COO$^-$ and O-H groups on SA molecules had been chemically crosslinked between the -COO$^-$ and O-H groups on SA molecules and the –COOH of CA.

5.4.3 X-ray Diffractometer

The amount of crystallinity of SA hydrogels was characterized by a XRD technique. Figure 5.2 [A] shows the diffraction peaks before and after the crosslinking process of SA hydrogels. It can be observed that, the crystallinity of SA hydrogel decreases after crosslinking by $CaCl_2$ and CA because crosslinking inhibites the SA chain packing (Li *et al.*, 2007).

Moreover, the crystallinity of SA hydrogels with the covalent crosslinking (Figure 5.3 [A] (c)) is higher than the ionic crosslinking method (Figure 5.3 [A] (b)), as evidenced by a shaper peak and a higher intensity of diffraction peak around 30°. This is because the chemical crosslinking agent provides greater molecular chains packing efficiency compared with the physical bonding (Gupta *et al.*, 2010). The order orientation of SA molecule obtained from the crosslinking with citric acid is also higher leading to a greater chain alignment and crystallinity.

Figure 5.3 [B] shows the diffraction peaks of PCB/HSA blends to compare the amount of PCB embedded in HSA hydrogels. The diffraction peak of SA hydrogel with adding PCB is shifted towards 45°, which is the diffraction peak of PCB (Gupta *et al.*, 2010). The crystallinity of PCB/HSA hydrogel blends decreases with increasing PCB concentration because of the inhibition of molecular chain packing of HSA by PCB (Li *et al.*, 2007 and Gupta *et al.*, 2010).

3.4 Thermal Gravimetric Analysis

The thermal behavior and the water content of SA hydrogels were characterized by TGA technique as shown in Table 5.2.

Table 5.2 shows the water contents of SA hydrogels with the ionic crosslinking and covalent crosslinking method. The data indicate an initial weight loss of approximately 90 wt% as temperature increases to 100°C, which corresponds to the desorption of bound water. In addition, the degradation of SA molecule occurs in the degradation temperature ($T_{d,onset}$) range of 200 - 230°C depending on molecular weight of SA.

Moreover, the weight loss of HSA hydrogels decreases with increasing PCB because of the Van der Waals force and the hydrogel bonding interaction between HSA and PCB (Pattavarakorn *et al.*, 2013). $T_{d,onset}$ of PCB/HSA

blends increases with increasing PCB because of higher $T_{d,onset}$ of PCB (Gupta *et al.*, 2010).

5.4.4 Scanning Electron Microscope

Figure 5.4 shows SEM micrographs of the PCB/HSA hydrogel blends of various PCB concentrations. PCB shows a moderate dispersion in the HSA hydrogel at low PCB concentration; the dispersion becomes relatively poor at high PCB concentration (concentration of PCB beyond 0.1 %v/v). Partially homogeneous PCB/HSA hydrogel blend is obtained because of the Van der Waals force and the hydrogen bonding interaction between PCB and HSA hydrogel (Tungkavet *et al.*, 2012).

5.4.5 Atomic Force Microscope

The phase separation in SA hydrogels of various crosslinking types was investigated by EFM technique as demonstrated in Figure 5.5. Figure 5.5 (a) shows a smooth phase with some small bright areas that refer to a low electrostatic force under applied electric field. The bright regions can be assigned to the presences of negative charges namely COO^- and OH^- on the HSA surface which provides the attractive force between the positively charged EFM tip and the negatively charged HSA surface.

For the HSA hydrogels with crosslinking process, a higher response to electric field is obtained, where the bright regions are more abundant as shown in Figure 5.5 (b) and 5.5 (c). Between the ionic and covalent crosslinking, the ionic crosslinking of $CaCl_2$ show continuously brighter areas (Figure 5.5 (b)) of like eggs shell block due to the formation of Ca^{2+} in HSA hydrogel (Kuen *et. al.*, 2012). In the case of covalent crosslinking, the existence of COO^- from CA is shown as the bright regions as well (Diana *et. al.*, 2012).

When HSA is added with PCB, the anionic phase becomes a more brilliant phase because PCB acting as a conductive polymer has more free electrons present (Figure 5.5 (d)) (Tungkavet *et al.*, 2012).

5.4.6 Time Dependence of the Electromechanical Response

The temporal characteristics of a HSA hydrogel by ionic crosslinking, a HSA hydrogel by covalent crosslinking; and a PCB/HSA hydrogel by ionic crosslinking at PCB concentration of 0.1 %v/v at electric field strength of 800 V/mm were investigated in which the electric field was turn on and off alternately at every 600 second. The temporal characteristic of each sample was recorded in the linear viscoelastic regime at a strain of 0.1 %, and frequency of 100 rad/s.

Figure 6 shows a comparison of the storage modulus (G') during the time sweep test. In all samples, G' increases rapidly when the electric field is on due to the polarization of HSA molecule (Tungkavet *et al.*, 2012), and decreases instantaneously when the electric field is off. They attain the steady state at different actuating cycles where the HSA hydrogel by ionic crosslinking takes 3 cycles, the HSA hydrogel by covalent crosslinking requires 2 cycles, but PCB/HSA takes only 1 cycle to reach the polarization equilibrium.

5.4.7 Electromechanical Properties

The electromechanical properties of SA hydrogels were characterized by the melt rheometer under oscillatory shear mode at 300K. The strain sweep tests were first carried out to determine an appropreate strain for measuring the storage modulus (G') in a linear viscoelastic regime. The appropriate strain value in the linear viscoelastic regime of 1%v/v HSA, 1%v/v MSA, and 1%v/v LSA hydrogel crosslinked with 0.015%v/v $CaCl_2$ was around 0.1%. The appropriate strain value in the linear viscoelastic regime of 1 %v/v HSA, 1%v/v MSA, and 1%v/v LSA hydrogel crosslinked with 0.50 %v/v CA was around 0.1%.

Figure 5.7 shows the storage moduli (G') and storage modulus sentivities ($\Delta G'/G'_o$) vs. electric field of 1%v/v HSA crosslinked by 0.015 %v/v $CaCl_2$ and crosslinked by 0.50%v/v CA, respectively, at frequency 100 rad/s and at 300 K. The data clearly show that when the electric field is introduced into the system, the G' of the samples increases because the electrostatic interactions between induced dipole moments on the alginate chain occur leading to the intermolecular interaction similar to an electrical network (Niamlang *et al.*, 2008; Hiamtup *et al.*, 2008; Tungkavet *et al.*,2012; and Kunchornsupand *et al.*, 2014). In

other words, the SA hydrogels become polarized and dipole moments are generated. This in turn reduces the chain free movements and enhance the chain rigidity. Moreover, the G' of the samples increase with increasing the molecular weight of SA as shown in Table 5.3. As the molecular weight of alginate increases, the number of carboxylic groups or dipole moments increases leading to a stronger interaction under applied electric field (Kunanuruksapong *et al.*, 2008; Thipdech *et al.*, 2008; Tungkavet *et al.*, 2012; and Niamlangand *et al.*, 2013). However, the loss modulus (G″) increased with increasing electric field strength and SA molecular weight due to the polarization of water ions and hydrogen bonding between SA and water (Thonksak *et al.*, 2012).

At electric field of 800 V/mm, the highest molecular weight SA showed the highest $\Delta G'/G'_0$ values namely 7.5 and 5.5 for ionic crosslink and covalent crosslink, respectively. But for the lowest molecular weight, the $\Delta G'/G'_0$ values for the ionic crosslink and covalent crosslink were 3.3 and 2, respectively. From this result, it can be concluded that a higher molecular weight containing a larger amount of polar groups provides a better electromechanical response compared to those of the low molecular weight.

For the storage modulus sensitivity ($\Delta G'/G'_o$) of SA from ionic crosslinking and covalent crosslinking, the storage modulus sensitivity of the ionic crosslinking is higher than the covalent crosslinking because the ionic crosslinking is a physical interaction and the dipoles and ions are easier to move or rotate within the specimen. The covalent crosslinking is a chemical interaction between the carboxylic group of SA and the carboxyl group of citric acid (Kunchornsup *et al.*, 2010 and Tungkavet *et al.*, 2012). The polar groups of SA are restricted in movement leading to a lower electromechanical response (Tungkavet *et al.*, 2012).

In comparison with other electroactive polymers, the styrene-isoprene-styrene triblock (D114P, D1164P, D1162P) exhibited the storage modulus sensitivity of 0.122, 0.102, and 0.050 (Thonksak *et al.*, 2012), the uncrosslinked high-gel-strength gelatin exhibited the storage modulus sensitivity of 2.30 (Thwatchai *et al.*, 2012). Both types of the crosslinked SA hydrogels possess the superior responses and sensitivity values which are an order of magnitude greater than those triblock polymers and gelatin, as shown in Table 5.3.

Figure 5.8 shows the storage modulus sentivity ($\Delta G'/G'_o$) vs. electric field of PCB/PCB/HSA blends by ionic crosslinking (0.015 %v/v $CaCl_2$) of various PCB concentrations of 0.01 %v/v, 0.05 %v/v, 0.10 %v/v, 0.03 %v/v, and 0.50 %v/v, respectively, at frequency of 100 rad/s and at 300 K. The data show that when the PCB is introduced into the system at 0.01 %v/v, 0.05 %v/v, and 0.10 %v/v, the storage modulus increases at a given electric field strength. The highest $\Delta G'/G'_o$ obtained is 18.55 from the 0.10 %v/v PCB/HSA blend. This is because the PCB acts as a conductive polymer which produces additional dipole moments and enhencs the electron mobility within the PCB/HSA hydrogel blends (Ludeelerd *et al.*, 2010; Tangboriboon *et al.*, 2010; Tangboriboon *et al.*, 2011; Tungkavet *et al.*, 2012; and Tangboriboonand *et al.*, 2013). At PCB concentrations higher than 0.10 %v/v PCB, the $\Delta G'/G'_o$ decreases at a given electric field strength because of the phase separation between PCB and HSA or the PCB aggregation obstructs the dipole moment interaction within the specimen (Chotpattananont *et al.*, 2006; Tangboriboon *et al.*, 2011; Tungkavet *et al.*, 2012; and Tangboriboon *et al.*, 2012).

5.4.8 Deflection Responses

The deflection of the HSA hydrogel by ionic crosslinking; covalent crosslinking; and PCB/HSA hydrogel blends was studied by vertically suspending the hydrogels in a silicone oil bath. The electric deflection responses of HSA hydrogel and 0.10 %v/v PCB/HSA hydrogel blend with and without an electric field strength of 500 V/mm are shown in Figure 5.9. Upon applying an electric field, the free lower ends of the hydrogels deflect toward the positive electrode, with the amounts depending on the electric field strength, Thedeflection responsessuggest an attractive interaction between the positive electrode charge and the polarized carboxyl and hydroxyl group, in which the HSA structures possesse net negative charge. Another mechanism for the deflection also arises from the dieletrophoresis force originated from polarizable body in a nonuniform electric field (Petcharoen *et al.*, 2013).The deflection distances, deflection angles and dielectrophoretic forces of the HSA hydrogel and the PCB/HSA hydrogel blend are shown in Figure 5.10 and Table 5.4. The HSA hydrogel shows a greater deflection distance value and deflection angle than the PCB/HSA hydrogel blends. However, the HSA/PCB

hydrogel blends show a higher dielectrophoretic forces at a given electric field strength relative to the HSA hydrogel. The highest dielectrophoretic forces occur with the 0.1 %v/v PCB because PCB acts as a conductive polymer producing additional dipole moments and enhancing the electron mobility within the PCB/HSA hydrogel composite (Niamlanget *al.*, 2008 and Tungkavet *et al.*, 2012). At a higher PCB concentration, the dielectrophoretic force decreases because of the PCB aggregation reducing polarizability (Tungkavet *et al.*, 2011and Kunanuruksapong *al.*, 2011). Whereas the deflection distance and deflection angle decrease because of the higher initial rigidity and the PCB agglomoration (Tungkavet *et al.*, 2011). The dielectrophoretic forces at the electric field strength of 500 V/mm of the HSA, 0.01 %v/v PCB/HSA, 0.05 %v/v PCB/HSA, 0.10 %v/v PCB/HSA, 0.50 %v/v PCB/HSA, 0.10 %v/v PCB/HSA, 0.30 %v/v PCB/HSA, and 0.50 %v/v PCB/HSA hydrogel blends are 1.00, 1.78, 1.83, 2.76, 2.18 and 1.06 mN, respectively.

In comparison with the previous work, the maximum dielectrophoretic force at 500 V/mm of styrene-isoprene-styrene triblock copolymer (D1114P) was 20.5 μN (Thonksak *et al.*, 2010).The dielectrophoretic force of a gelatin hydrogel at 600 V/mm was 7.05 mN (Tungkavet *et al.*, 2012). The dielectrophoretic force of a cellulosic gel at 500 V/mm was 4.63 mN (Kunchornsup *et al.*, 2012).

5.5 Conclusions

The electromechanical properties and the cantilever bending of the SA hydrogels and PCB/HSA hydrogel blends were investigated at electric field strength varying from 0-800 V/mm. For the SA hydrogels, the storage modulus response ($\Delta G'$) and the storage modulus sensitivity ($\Delta G'/G'_0$) increased dramatically with increasing electric field strength. The $\Delta G'$ and $\Delta G'/G'_0$ of SA hydrogels with ionic crosslinking were higher than those of the SA hydrogels with covalent crosslinking. Moreover, the $\Delta G'$ and $\Delta G'/G'_0$ of the SA hydrogels increased with increasing molecular weight of SA.

For the PCB/HSA hydrogel composites, The $\Delta G'/G'_0$ increased with increasing PCB concentration; it was the highest with the 0.10%v/v PCB/HSA, and it decreased at PCB concentrations higher than 0.10%v/v.

In the deflection measurement, the deflection distances and the dielectrophoretic forces of the HSA hydrogel and PCB/HSA hydrogel blends increased monotonically with increasing electric field strength. The PCB/HSA hydrogel blends showed higherdielectrophoretic forces but lower dflection distances relative to those those of the HSA hydrogel.

5.6 Acknowledgements

The work received financial supports from the Conductive and Electroactive Polymers Research Unit (CEAP) of Chulalongkorn University, the Thailand Research Fund (TRF), and the Royal Thai Government.

5.7 References

Pattavarakorn, D., Youngta, P., Jaesrichai, S., Thongbor, S., and Chaimongkol, P. (2013) Electroactive Performances of Conductive Polythiophene/Hydrogel Hybrid Artificial Muscle. Energy Procedia, 34, 673–681.

Gupta, B., Singh, A.K., and Prakash, R. (2010) Electrolyte effects on various properties of polycarbazole. Thin Solid Films, 519, 1016-1019.

Harun, M.H., Saion, E., Kassim, A., Yahya, N., and Mahmud, E. (2007) Conjugated conducting polymers: A brief overview. JASA, 2, 63-68.

Hiamtup, P., Sirivat, A., and Jamieson, A.M. (2008) Electromechanical response of a soft and flexible actuator based on polyaniline particles embedded in a cross-linked poly(dimethyl siloxane) network. Materials Science and Engineering C, 28, 1044-1051.

Kuen, Y.L., and Mooneya, D.J. (2012) Alginate: Properties and biomedical applications. Polymer Science, 37, 106–126.

Kulkarni, A.R., Soppimath, K.S., Aminabhavi, T.M., Dave, A.M., and Mehta, M.H. (2000) Glutaraldehyde crosslinked sodium alginate beads containing liquid pesticide for soil application. Controlled Release, 63, 97-105.

Kunanuruksapong, R., and Sirivat, A. (2008) Electrical properties and electromechanical responses of acrylic elastomers and styrene copolymers: effect of temperature. Applied Physics A, 92, 313-320.

Kunanuruksapong, R., and Sirivat, A. (2011) Effect of dielectric constant and electric field strength on dielectrophoresis force of acrylic elastomers and styrene copolymers. Current Applied Physics, 11, 393-401.

Kunchornsup, W., and Sirivat, A. (2012) Physically cross-linked cellulosic gel via 1-butyl-3-methylimidazolium chloride ionic liquid and its electromechanical responses. Sensors & Actuators A, 175, 155-164.

Kunchornsup, W., and Sirivat, A. (2010) Effects of crosslinking ratio and aging time on properties of physical and chemical cellulose gels via1-butyl-3-methylimidazolium chloride solvent. Sol-Gel Science and Technology, 56, 19-26.

Kunchornsup, W., and Sirivat, A. (2014) Electromechanical properties study of 1-butyl-3-methylimidazolium chloride/cellulosic gel blended with polydiphenylamine. Sensors and Actuators A: Physical, 220, 249–261.

Liangbin Li, Yapeng Fang, Rob Vreeker, and Ingrid Appelqvist. (2007) Reexamining the Egg-Box Model in Calcium−Alginate Gels with X-ray Diffraction. Biomacromolecules, 8, 464-468.

Ludeelerd, P., Niamlang, S., Kunaruksapong, R., and Sirivat, A. (2010) Effect of elastomer matrix type on electromechanical response of conductive polypyrrole/elastomer blends. Physics and Chemistry of Solids, 71, 1243-1250.

Mirfakhrai, T., Madden, D. W., and Baughman, R. H. (2007) Polymer artificial muscles. Material Today, 10, 30-38.

Niamlang, S., and Sirivat, A. (2008) Electromechanical responses of a crosslinked polydimethylsiloxane. Macromolecular Symposia, 264, 176-183.

Niamlang, S., and Sirivat, A. (2008) Dielectrophoresis force and deflection of electroactive poly(p-phenylene vinylene)/polydimethylsiloxane blends. Smart Materials and Structures, 17, 035036(1-8).

Paradee, N., and Sirivat, A. (2013) Synthesis of poly(3,4-ethylene- dioxythiophene) nanoparticles via chemical oxidation polymerization. Poly Int, 63, 106–113.

Petcharone K. and Sirivat A. (2013) Electroactive properties of thermoplastic polyurethane elastomer: Effects of urethane type and soft-hard segment composition. Current Applied Physics, 13, 1119-1127.

Puvanatvattana, T., Chotpattananont, D., Hiamtup, P., Niamlang, S., Sirivat, A., and Jamieson, A.M. (2006) Electric field induced stress moduli in polythiophene/ polyisoprene elastomer blends. Reactive and Functional Polymers, 66, 1575-1588.

Raj, V., Madheswari, D., and Ali, M. (2010) Chemical formation, characterization and properties of polycarbazole. Applied Polymer Science, 116, 147-154.

Tangboriboon, N., Uttanawanit, N., Longtong, M., Wongpinthong, P., Sirivat, A., and Kunanuruksapong, R. (2010) Electrical and electrorheological properties of alumina/ natural rubber (STR XL) composites. Materials, 3, 656-671.

Tangboriboon, N., Longtong, M., Sirivat, A., and Kunanuraksapong, R. (2011) Electrical and electromechanical properties of alumina/natural rubber STR 5L composites. Materials Technology, 26, 100-106.

Tangboriboon, N., Datsanae, S., Onthong, A., Kunanuruksapong, R., and Sirivat, A. (2013) Electromechanical responses of dielectric elastomer composite actuators based on natural rubber and alumina. Elastomers & Plastics, 45, 143- 161.

Tangboriboon, N., Mulsow, L., Kunchornsup, W., and Sirivat, A. (2013) Ceramic granules forming from calcium sodium aluminosilicate and carboxymethyl cellulose. Ceramic Processing Research, 14, 658-666.

Tungkavet, T., Sirivat, A., Seetapan, N., and Pattavarakorn, D. (2013) Stress relaxation behavior of (Ala-Gly-Pro-Arg-Gly-Glu-4Hyp-Gly-Pro-) gelatin hydrogels under electric eld: Time-electric field superposition. Polymer, 54, 2414-2421.

Table 5.1 Crosslinking density (mol/cm^3) of SA hydrogels of various $CaCl_2$ and CA concentrations

SA Types (1%v/v)	Ionic Crosslinking		Covalent Crosslinking	
	$CaCl_2$ Concentrations (%v/v)	Crosslinking Density $(mol/cm^3)\times10^6$	CA Concentrations (%v/v)	Crosslinking Density $(mol/cm^3)\times10^6$
HSA	0.0050	10.36 ± 2.33	0.25	-
	0.0100	14.70 ± 6.28	0.50	19.79 ± 8.78
	0.0150	18.50 ± 8.87	0.75	74.34 ± 12.65
	0.0200	19.80 ± 7.31	1.00	165.8 ± 14.26
MSA	0.0050	11.47 ± 0.58	0.25	-
	0.0100	12.06 ± 0.04	0.50	15.60 ± 2.77
	0.0150	16.71 ± 1.20	0.75	63.82 ±8.16
	0.0200	21.01 ± 2.00	1.00	156.23 ± 28.32
LSA	0.0050	12.66 ± 0.21	0.25	-
	0.0100	14.43 ± 0.72	0.50	20.82 ± 9.78
	0.0150	22.31 ± 9.46	0.75	60.23 ± 9.64
	0.0200	38.78 ± 0.24	1.00	132.76 ± 26.54

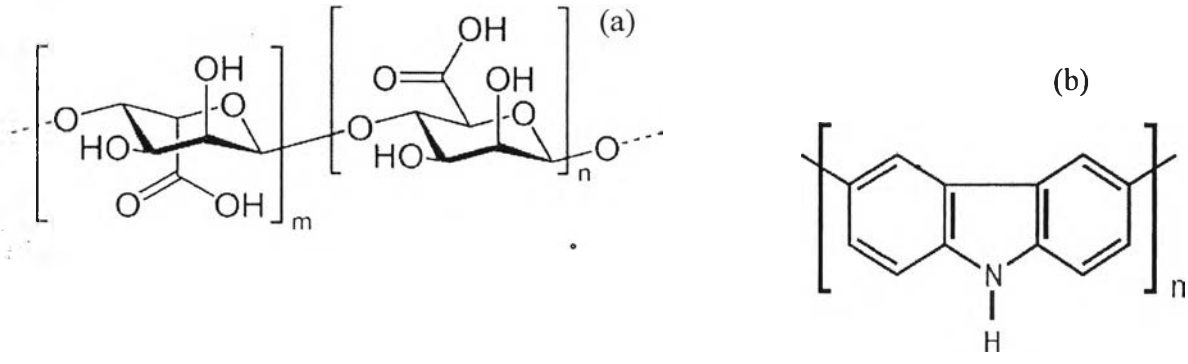

Figure 5.1 Chemical Structures of: (a) SA; (b) PCB

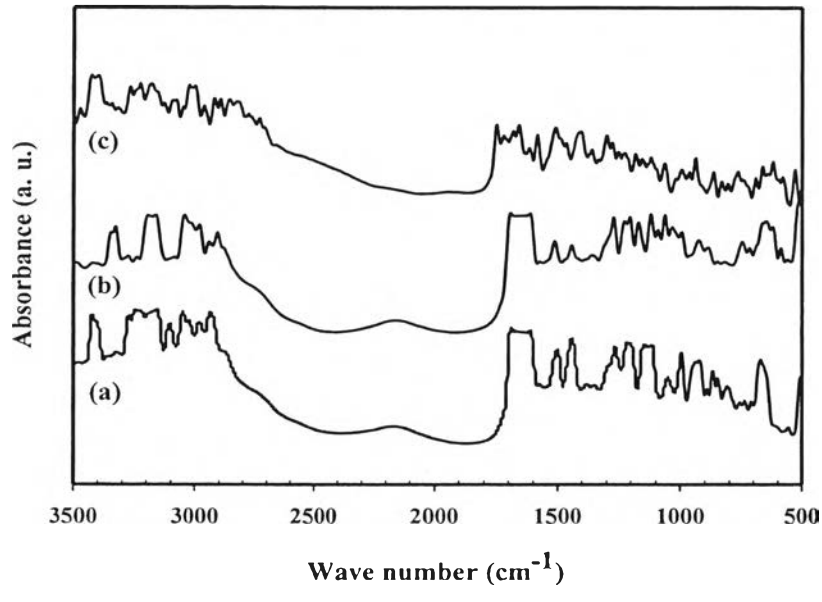

Figure 5.2 FTIR spectra of SA hydrogels: (a) pristine 1%v/v HSA; (b) 1%v/v HSA + 0.015%vlv $CaCl_2$; and (c) 1%v/v HSA + 0.50%vlv CA.

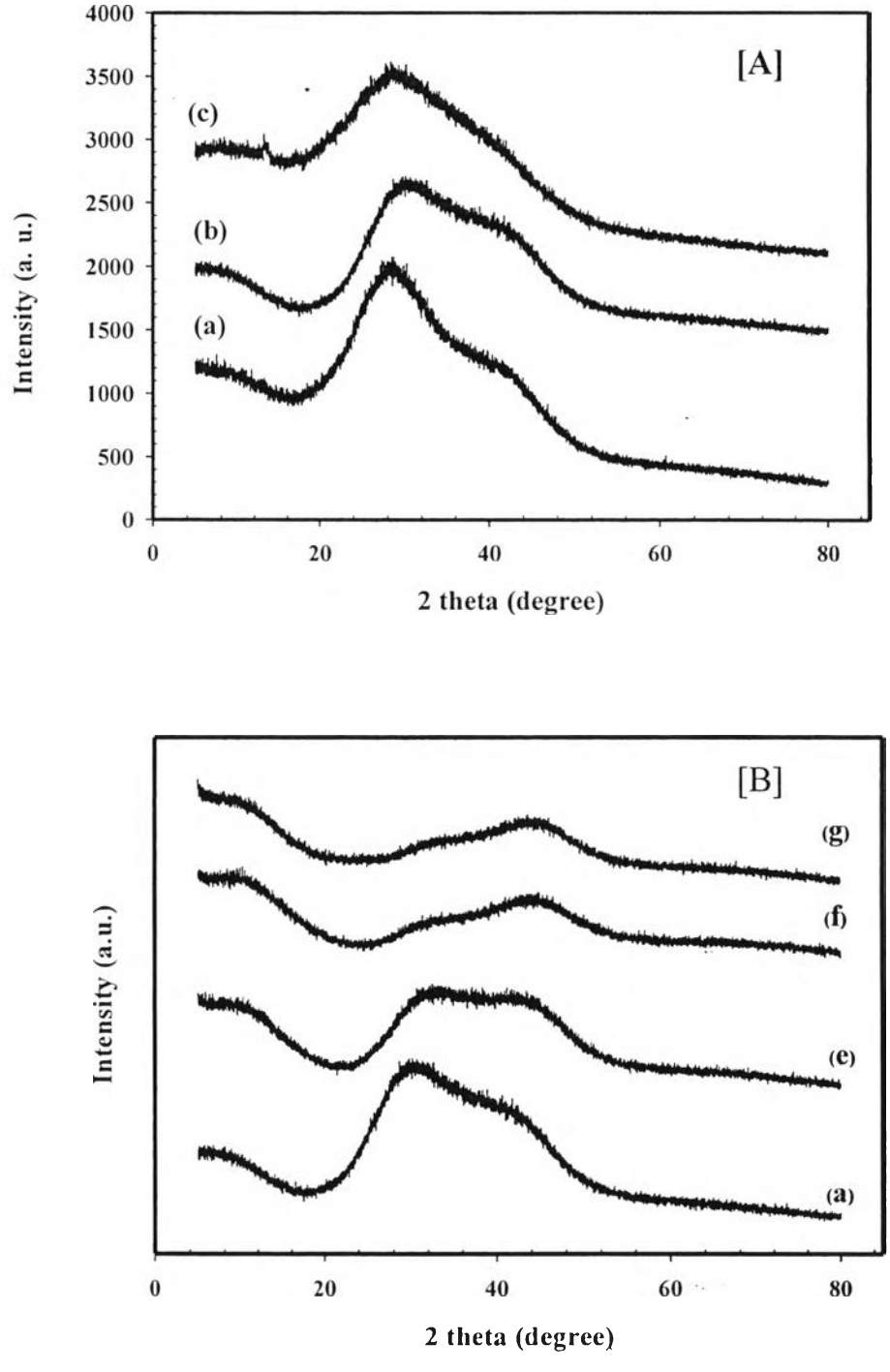

Figure 5.3 XRD diffraction peaks of [A] HSA hydrogesl: (a) pristine HSA; (b) 1 %v/v HSA + 0.015 %v/v $CaCl_2$; and (c) 1 %v/v HSA+ 0.50 %v/v CA and [B] PCB/HSA hydrogel blends by ionic crosslinking method: (a) pristine HSA; (e) 0.01 %v/v PCB/HSA; (f) 0.05 %v/v PCB/HSA; and (g) 0.10 %v/v PCB/HSA.

Table 5.2 Degradation temperatures and percent weight lossed from TGA thermograms of pristine SA hydrogels and blends.

Sample	Water Content (%)	Weight Loss (%)	$T_{d,onset}$ (°C)
1%v/v HSA + 0.015%v/v $CaCl_2$	93.15	97.95	215
1%v/v MSA + 0.015%v/v $CaCl_2$	93.17	97.77	209
1%v/v LSA + 0.015%v/v $CaCl_2$	94.95	97.35	201
1%v/v HSA + 0.5%v/v CA	89.45	86.25	227
1%v/v MSA + 0.5%v/v CA	90.32	87.67	220
1%v/v LSA by + 0.5%v/v CA	91.78	88.98	210
0.01%v/v PCB/HSA + 0.015%v/v $CaCl_2$	93.45	92.07	239
0.05%v/v PCB/HSA + 0.015%v/v $CaCl_2$	92.93	88.43	248
0.10%v/v PCB/HSA + 0.015%v/v $CaCl_2$	92.40	88.07	250
0.30%v/v PCB/HSA + 0.015%v/v $CaCl_2$	92.13	87.66	252
0.50%v/v PCB/HSA + 0.015%v/v $CaCl_2$	89.82	83.74	257

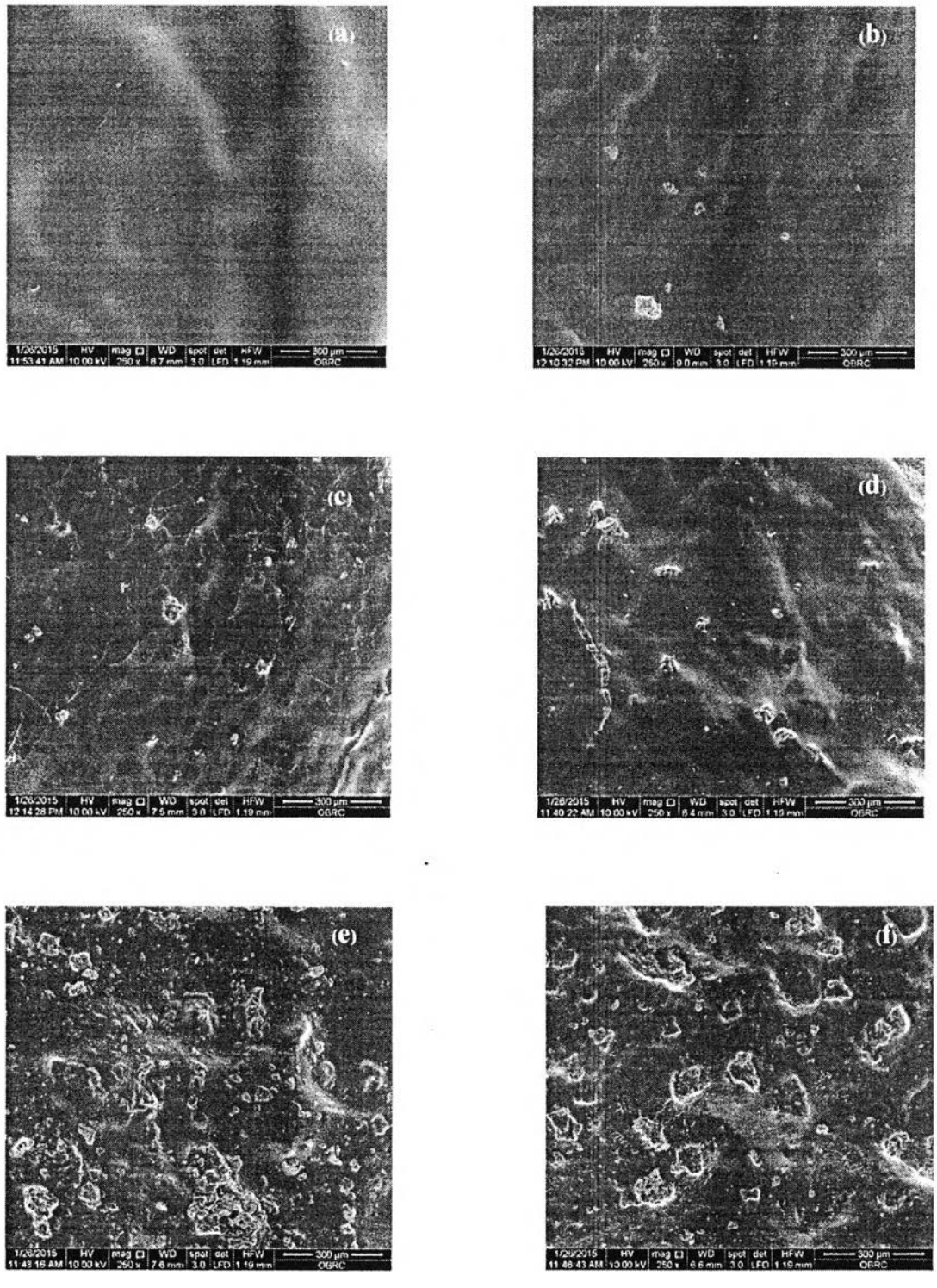

Figure 5.4 SEM photographs of PCB/HSA hydrogel blends of various PCB concentrations: (a) pristine HSA; (b) 0.01%v/v PCB; (c) 0.05%v/v PCB; (d) 0.10%v/v; (e) 0.30%v/v PCB; and (f) 0.50%v/v PCB.

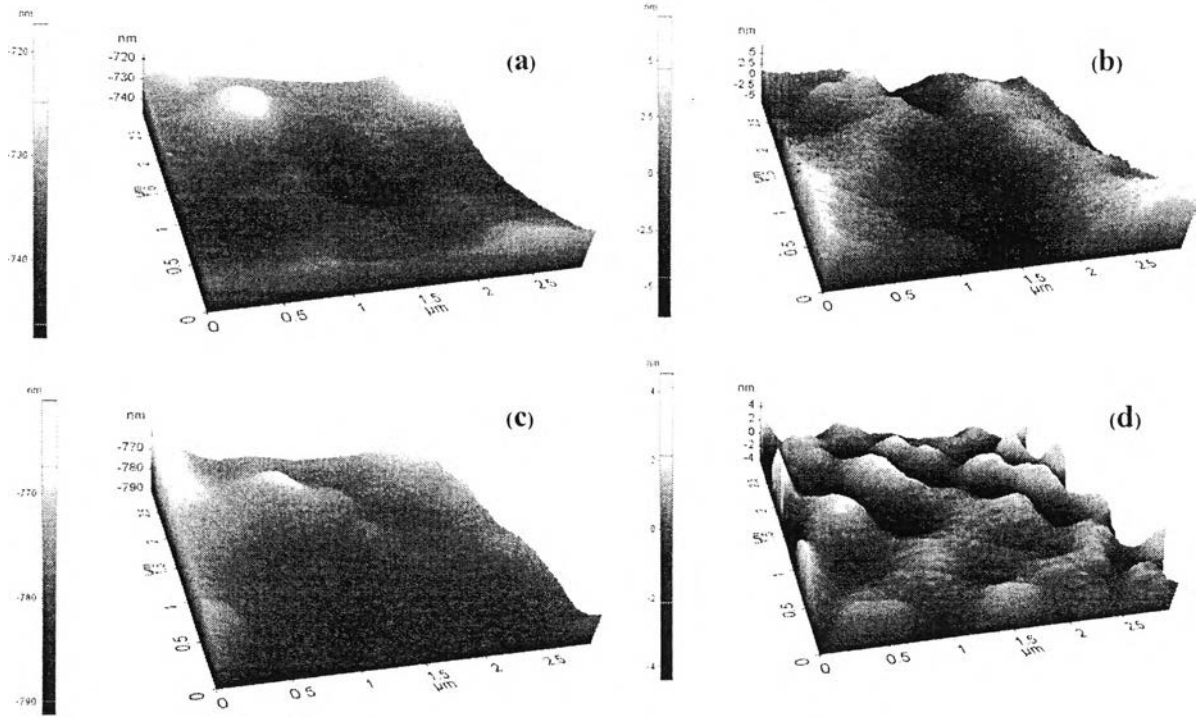

Figure 5.5 EFM images ($2.5\times2.5\mu m^2$): (a) HSA without crosslinking; (b) 1 %v/v HSA + 0.015 %v/v $CaCl_2$; (c) 1 %v/v HSA + 0.50 %v/v CA; and (d) 0.01%v/v PCB/HSA + 0.015 %v/v $CaCl_2$ hydrogel blend.

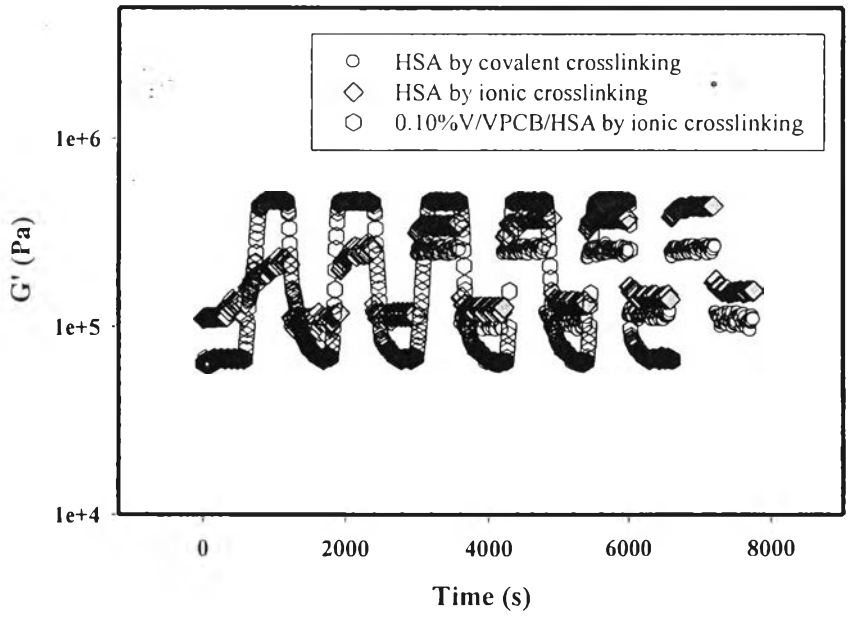

Figure 5.6 Temporal response of 1%v/v HSA hydrogels and 0.1%v/v PCB/HSA hydrogel blends at frequency of 100 rad/s, electric field strength of 800 V/mm, and at 300 K.

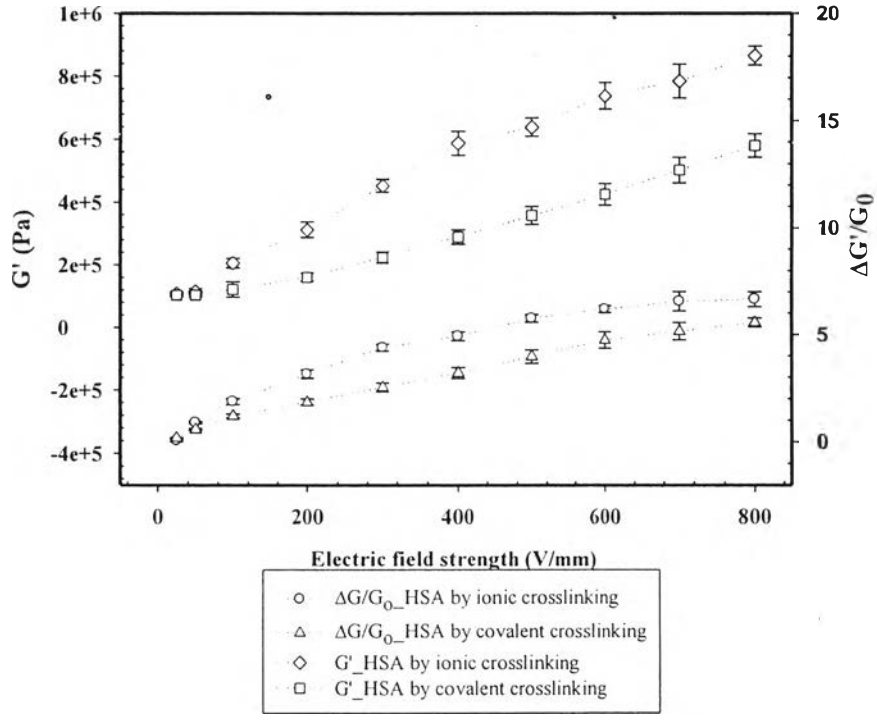

Figure 5.7 The storage modulus (G') and storage modulus sensitivity ($\Delta G'/G'_o$) versus electric field strength of 1%v/v HSA at strain of 0.1 %, frequency of 100 rad/s, and at 300 K.

Table 5.3 Comparison of storage modulus sensitivities ($\Delta G'/G'_o$) of SA hydrogels and electroactive materials

Material	Electric Field Strength (kV/mm)	Frequency (rad/s)	Storage Modulus Sensitivity ($\Delta G'/G'_o$)	Reference
1%v/v HSA + 0.015%v/v $CaCl_2$	0.8	100	7.48	-
1%v/v HSA + 0.50%v/v CA			5.50	-
Styrene-isoprene-styrene triblock (D1114P)	1	1	0.122	Thonksak *et al.*,2010
Styrene-isoprene-styrene triblock (D1164P)			0.102	
Styrene-isoprene-styrene triblock (D1162P)			0.050	
Uncrosslinked high-gel-strength gelatin	1	100	2.30	Thonksak *et al.*,2012
3% crosslinked high-gel-strength gelatin			0.49	

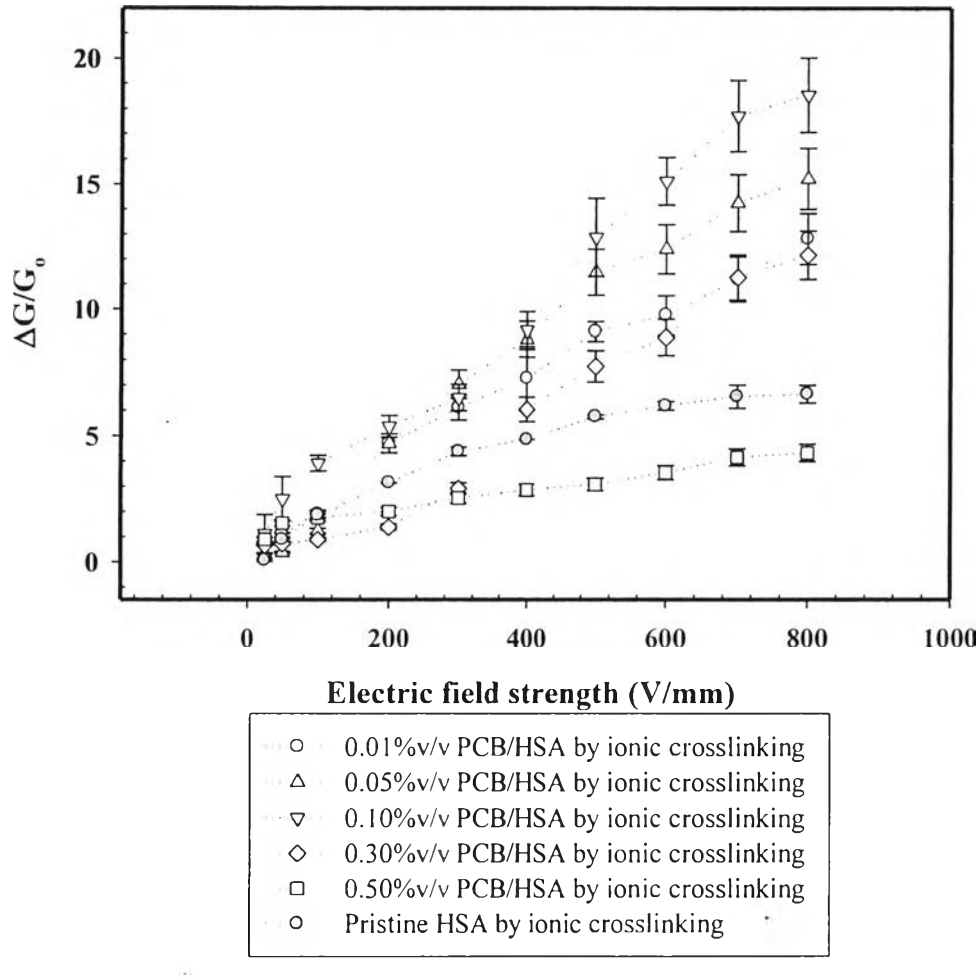

Figure 5.8 The storage modulus sensitivity ($\Delta G'/G'_o$) versus electric field strength of pristine HSA and PCB/HSA hydrogel blend at strain of 0.1 %, frequency of 100 rad/s, and at 300 K.

Table 5.4 Comparison of electromechanical properties of the SA hydrogels at frequency of 100 rad/s, electric field strength of 800 V/mm, and at 300 K

Material	Initial Storage Modulus (G'_0, Pa)	Storage Modulus (G', Pa)	Storage Modulus Sensitivity ($\Delta G'/G'_0$)
1%v/v HSA + 0.015%v/v $CaCl_2$	$1.09\times10^5 \pm 1.49\times10^4$	$8.16\times10^5 \pm 3.81\times10^4$	7.66 ± 0.35
1%v/v MSA + 0.015%v/v $CaCl_2$	$8.58E\times10^4 \pm 3.07\times10^3$	$5.35\times10^5 \pm 2.41\times10^4$	6.20 ± 0.28
1%v/v LSA + 0.015%v/v $CaCl_2$	$2.51\times10^4 \pm 9.38\times10^3$	$2.51\times10^5 \pm 9.38\times10^3$	3.37 ±0.33
1%v/v HSA + 0.50%v/v CA	$1.10\times10^5 \pm 6.69\times10^3$	$6.89\times10^5 \pm 5.51\times10^4$	5.36± 0.43
1%v/v MSA + 0.50%v/v CA	9.50E+04 ± 7.60×10^3	$6.10\times10^5 \pm 4.88\times10^4$	5.02 ± 0.40
1%v/v LSA + 0.50%v/v CA	$9.76\times10^4 \pm 7.81\times10^3$	$3.06\times10^5 \pm 9.38\times10^3$	2.12 ± 0.17
0.01%v/v PCB/HSA + 0.015%v/v $CaCl_2$	$3.22\times10^4 \pm 2.57\times10^3$	$4.44\times10^5 \pm 3.55\times10^4$	12.80 ± 1.02
0.05%v/v PCB/HSA + 0.015%v/v $CaCl_2$	$3.25\times10^4 \pm 2.60\times10^3$	$5.27\times10^5 \pm 4.22\times10^4$	15.21 ± 1.22
0.10%v/v PCB/HSA + 0.015%v/v $CaCl_2$	$3.30\times10^4 \pm 2.64\times10^3$	$6.26\times10^5 \pm 5.01\times10^4$	18.55 ± 1.48
0.30%v/v PCB/HSA + 0.015%v/v $CaCl_2$	$3.32\times10^4 \pm 2.66\times10^3$	$4.21\times10^5 \pm 3.37\times10^4$	12.15 ± 0.97
0.50%v/v PCB/HSA + 0.015%v/v $CaCl_2$	$5.02\times10^4 \pm 4.01\times10^3$	$1.44\times10^5 \pm 1.15\times10^4$	4.33 ± 0.35

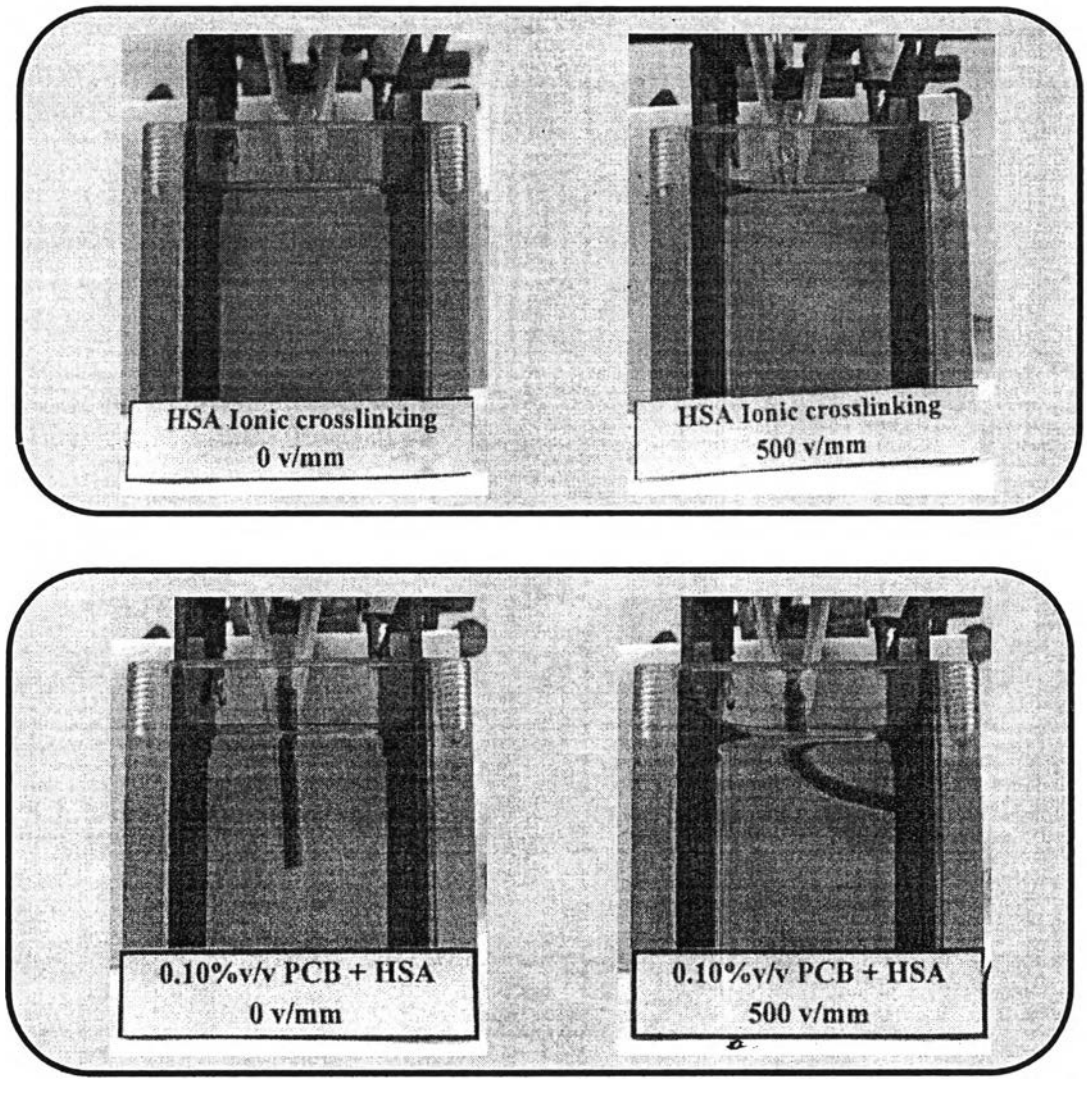

Figure 5.9 Bending of pristine HSA hydrogel and 0.10%v/v PCB/HSA hydrogel blend at electric field strength 0 and 500 v/mm.

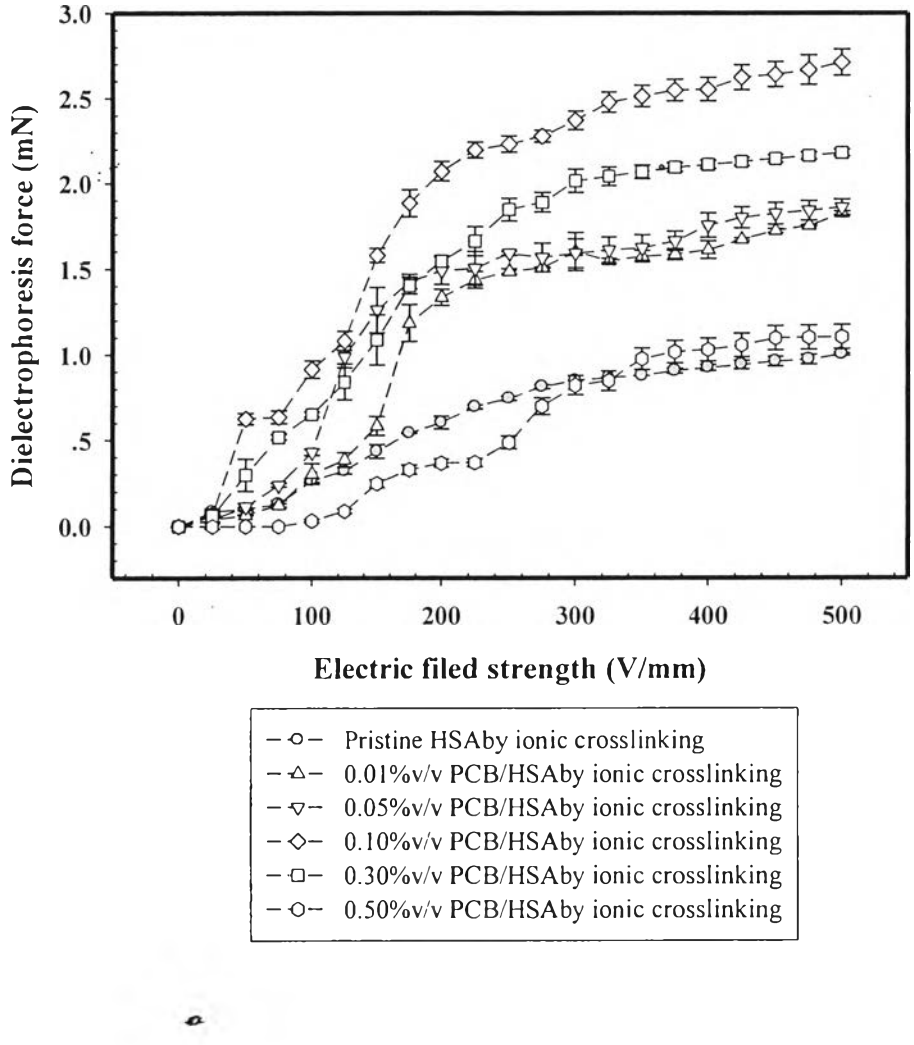

Figure 5.10 Dielectrophoresis force (F_d) versus electric field strength of pristine HSA and PCB/HSA hydrogel blend.

Table 5.5 Deflection angles, deflection distances, and dielectrophoresis forces of PCB/HSA composites with at electric field strength of 500 V/mm

Materials	Deflection Angle (Degree)	Deflection Distance (mm)	Dielectrophoresis Force (mN)
1 %v/v HSA + 0.015 %v/v $CaCl_2$	55.58 ± 0.23	18.10 ± 0.57	1.00 ± 0.01
1 %v/v HSA + 0.50 %v/v CA	46.15 ± 0.39	15.31± 0.42	0.75 ± 0.02
0.01 %v/v PCB/HSA + 0.015 %v/v $CaCl_2$	40.11 ± 1.76	14.00 ± 0.99	1.78 ± 0.17
0.05 %v/v PCB/HSA + 0.015 %v/v $CaCl_2$	40.34 ± 1.64	14.35 ± 0.35	1.83 ± 0.01
0.10 %v/v PCB/HSA + 0.015 %v/v $CaCl_2$	44.19 ± 0.13	15.75 ± 0.07	2.76 ± 0.15
0.30 %v/v PCB/HSA + 0.015 %v/v $CaCl_2$	36.69 ± 2.85	12.60 ± 0.99	2.18 ± 0.02
0.50 %v/v PCB/HSA + 0.015 %v/v $CaCl_2$	24.29 ± 0.17	8.89 ± 0.07	1.06 ± 1.16